inter.noise
27-30 AUGUST HONG KONG 2017

Experimental and numerical investigation of enclosed cavity noise in the presence of interior trim materials

Zhengqing LIU[1]; Mohammad FARD[2]; John Laurence DAVY[3]; Takuya YOSHIMURA[4]

[1, 2] School of Engineering, RMIT University, Australia

[3] School of Science, RMIT University, Australia

[4] Department of Mechanical Engineering, Tokyo Metropolitan University, Japan

ABSTRACT

This paper presents a rigid walled car cabin model to predict the acoustic effects of vehicle interior trim materials. The car cavity is made of a rigid walled enclosure system with one flexible wall on the front firewall position, where the interior trim materials are applied to the inner surface of the front firewall to modify the coupling between the flexible wall and the cabin air cavity. The car cabin is acoustically excited by using a single point source positioned at one corner of the inner air cavity to imitate the airborne noise. The propagated noise is measured by using pressure microphones at different locations inside the car cabin: one near the driver's ear position and another one near the passenger's ear position. An acoustic FE (Finite Element) model is also developed to investigate and predict the effects of interior trim materials on the car cabin noise level. Finally, the simulation results are compared with the experimentally acquired acoustic effects of the interior trim materials. The predicted acoustic response results show that the simulation agrees well with the experiment data, both with and without the interior trim materials. The noise propagating inside the car cabin is reduced by a similar ratio in both the experimental method and in the numerical analysis. The selected interior trim materials are starting to absorb noise at frequencies above 500 Hz, but they do not reduce the low-frequency noise effectively.

Keywords: Airborne noise propagation, Vehicle interior trim materials, Acoustic properties, Car cabin FE model I-INCE Classification of Subjects Number(s): 25; 35; 72; 76

1. INTRODUCTION

The control of vehicle interior cabin noise is a challenging task due to all the acoustic properties, vehicle safety and ride comfort that need to be satisfied. Among the existing solutions to reduce vehicle cabin noise level, passive noise control by using interior trim acoustic treatments (e.g. porous material) has a significant role in controlling both the structure-borne radiated noise and the airborne noise. The vehicle interior trim porous materials are used to increase the acoustic energy dissipation and to absorb the detrimental noise in the vehicle passenger compartment. Their physical mechanisms are mainly due to a viscous effect, a thermal effect, and a structural damping effect, by which the porous materials can transform the acoustic energy and vibration energy into heat energy.

The Finite Element (FE) method is usually used to reduce the vehicle interior noise based on acoustics and vibration measurements (1-5). However, the numerical prediction of the effects of the interior trim materials on vehicle cabin noise is complex and challenging. A simplified vibro-acoustic model such as a coupled plate and air cavity system were mostly used to replace a more complex vehicle structure modeled with the FE method. Early works modeling a coupled plate and cavity system were mainly reported by Dowell and Voss (6) and Dowell et al. (7), who developed a comprehensive modal-based theory to predict the interior sound field. The full

[1] liu.zhengqing@rmit.edu.au
[2] mohammad.fard@rmit.edu.au
[3] john.davy@rmit.edu.au
[4] yoshimu@tmu.ac.jp

theoretical solutions for the free and forced response of a vibro-acoustic coupled system was presented by Pretlove (8-10). The fundamental theories and experimental validations of the effect of vibro-acoustic coupling on sound waves in an enclosure have been well investigated and presented by Pan and Bies (11, 12), and Lee (13). Li et al. (14) studied a rectangular cavity coupled with a tilted wall, and the vibro-acoustic behavior of the coupled system was presented. Tanaka et al. (15) used a rectangular cavity with five rigid walls and a flexible plate to derive explicitly the eigenvalues of the cavity coupled system. Du et al. (16) have proposed a Fourier series method to analyze the acoustic properties of a rectangular cavity with general impedance boundary conditions, and with elastically restrained edges (17). The influence of the boundary conditions such as clamped and simply supported on the airborne sound insulation performance of a rectangular double plate was investigated by Xin and Lu (18). Moreover, a simplified vibro-acoustic coupled system was successfully used for vibration control (19), low-frequency noise control with micro-perforated panels (20) and for the optimization of the thickness of a multi-layered acoustic treatment (21).

The analytical study of the role of interior trim material on the noise control inside a coupled system was presented by Kang (22), Atalla et al. (23), and Bécot et al. (24, 25). They aimed to investigate the validity of the vibro-acoustic model in the case of a plate coated with a porous material and coupled to a rigid-walled cavity for the prediction of the acoustic response. An equivalent fluid model is usually used to model the porous material (26). It was mainly developed by Johnson et al. (27) and Champoux and Allard (28). The coupling between the structure, porous material, and the air cavity was presented by Atalla and Panneton (29). Liu et al. (30-32) develop a model to investigate the effect of the porous material on the noise inside an acoustic cavity generated by force excitation of one of the walls and validated the model by using the FEM.

The literature mentioned above provided several methods to predict the acoustic response of a plate cavity coupled system. However, there is limited experimentally validated data to predict the effects of the interior trim materials on vehicle cabin noise level. There is also little research on how porous material reduces the vehicle cabin noise due to acoustic excitation. This paper aims to present an experimentally validated car cabin model to characterize the acoustic effects of vehicle interior trims on acoustic excitation. An experimental method is first presented to generate the airborne noise and to measure the acoustic response inside the car cabin. An acoustic FE model is then used to predict the noise propagation from an acoustic source to receivers when the interior trim materials are present. Finally, the experiment data together with the predicted results are compared and discussed.

2. EXPERIMENT

2.1 Car cabin model

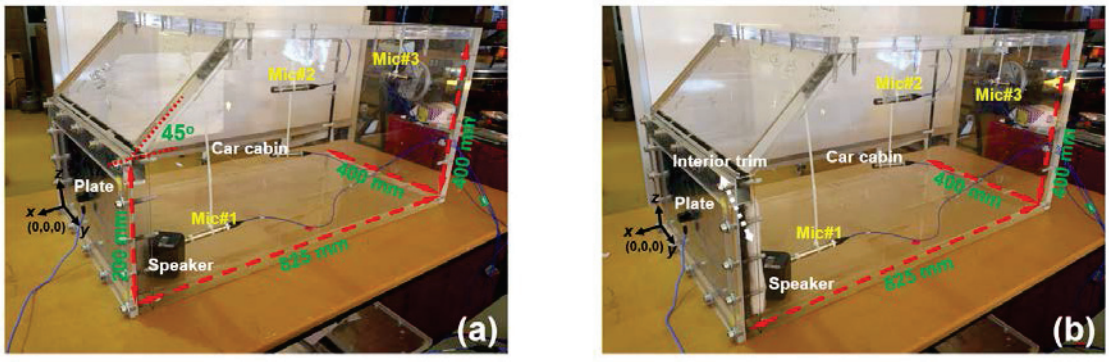

Figure 1 – Experiment setup in the laboratory: (a) a car cabin model without interior trim material; (b) a car cabin model with an interior trim material applied to the inner surface of the aluminum plate.

Figure 1 shows a scaled down car cabin model of a plate cavity system that was developed in the laboratory, and it was used to investigate the effect of the interior trim materials on the car cabin noise level (32). The car cabin was made of six rigid walls, and one simply supported flexible aluminum plate located in the front firewall position. The rigid walls were made of 25 mm Plexiglas to reduce the structure vibration and to ensure that the generated airborne noise was propagating only inside the car

cabin. The inner air cavity dimensions of the car cabin were 825 mm (x) × 400 mm (y) × 400 mm (z). The windshield has its lower end 200 mm above the floor with a 45° inclination angle such that the entire volume of the car cabin was 1.2×10^8 mm^3. The inner coupling area of the aluminum plate was 400 mm (y) × 200 mm (z), the thickness of the plate was 2.5 mm, and it was carefully bolted to the car cabin in the front firewall location all around its edges.

In this experiment, the inner air cavity was excited by a random acoustic signal (white noise) from a loudspeaker which was positioned in the corner of the car cabin. 1/2" random incidence, prepolarized condenser microphones (Model: 378B20; PCB Group, Inc.) were used to measure the Sound Pressure Level (SPL) inside the rigid walled car cabin. The LMS Data Acquisition System and LMS Test Lab (Siemens Product Lifecycle Management Software, Inc.) were utilized to acquire and process the acoustic signals from experimental data. An assumed local x-y-z coordinate system (coordinates in mm) and its origin point is also presented in Figure 1. Mic#1 was carefully hung inside the car cabin, and it was located at (–115, 335, 35) near the speaker to measure the sound source. The two receiver points inside the car cabin were Mic#2 (–340, 295, 290) and Mic#3 (–635, 305, 315). Mic#2 was used to measure the noise near the driver's ear position, and Mic#3 was used to measure the noise near the passenger's ear position.

2.2 Interior trim porous materials

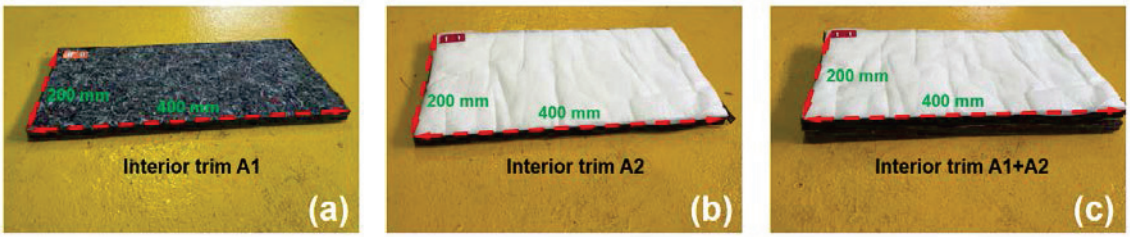

Figure 2 – Interior trim material samples used in this study: (a) Poly Felt non-woven material A1; (b) Polypropylene non-woven fabric material A2; (c) multilayer interior trim material A1+A2.

Figure 2 shows the prepared interior trim material samples used in this study. The interior trim material named A1 was mainly made from recycled polyester and cotton. The other interior trim material named A2 was mainly composed of a combination of polyester and polypropylene fibers with a double scrim layer. These two porous materials were commercially used on the vehicle interior trim acoustic package design, and they were provided by Futuris Automotive Interiors (Australia) Pty Ltd. The porous materials were cut down to 400 mm by 200 mm to fit the size of the aluminum plate. Their physical parameters and acoustic parameters were measured by Liu et al. (33), and they are listed in Table 1.

Table 1 – Physical properties and acoustical properties of the selected interior trim materials

Parameters	Interior trim material A1	Interior trim material A2
Average thickness, t (mm)	10.5	15.5
Average density, ρ_p (kg/m^3)	134.05	25.97
Air flow resistivity, σ (N.s/m^4)	131563	118587
Tortuosity, α_∞	1.1	1.7
Porosity, ϕ	0.989	0.829
Viscous characteristic length, Λ (μm)	192	127
Thermal characteristic length, Λ' (μm)	384	254

The following cases were studied to understand the influence of the interior trim materials on the noise level inside the car cabin. One case had the interior trim material applied to the inner surface of

the aluminum plate, and the other had no interior trim material. Moreover, a multilayer interior trim structure which combined A1 with A2 was also prepared and measured in this experiment. The interior trim material samples were carefully laminated on the inner surface of the aluminum plate, and the aluminum plate-backed porous material was then carefully bolted to the car cabin all around the edges of the plate. The airborne noise propagation inside the car cabin was measured at the same microphone (Mic#1, Mic#2 and Mic#3) locations with and without the porous interior trim material.

3. SIMULATION

3.1 Theoretical formulations

A coupled plate and cavity system treated with an interior trim material is considered in this study. Figure 3(a) shows the schematic diagram of a model for a car cabin treated with a porous material that is composed of three different components. They are the elastic part for a flexible plate, a porous material, and the acoustic cavity for the air-filled car cabin. It should be noted that the edges all around the flexible plate are assumed to be simply supported boundary conditions (18) and all other surrounding walls are assumed to be acoustically rigid. The classical formulations are used to model the plate and acoustic air cavity (15-17), and the porous material is modeled using the equivalent fluid formulations (27-29).

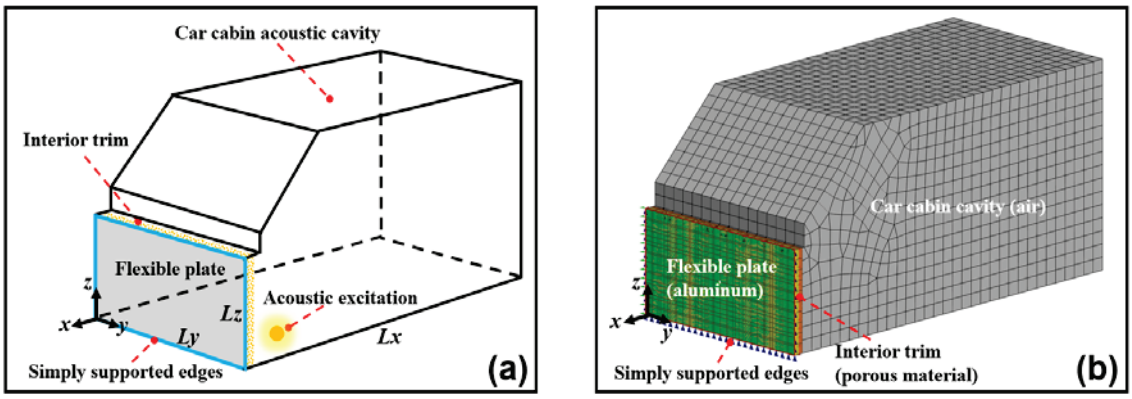

Figure 3 – (a) schematic diagram of a car cabin model of plate and cavity system with an interior trim material; (b) the developed acoustic FE model of a car cabin with interior trims (acoustic excitation).

Assume that the air in the car cabin is compressible and inviscid. The acoustic pressure inside the rigid car cabin satisfies the classical wave equation given by:

$$\nabla^2 p(x,y,z,t) - \frac{1}{c_0^2}\frac{\partial^2 p(x,y,z,t)}{\partial t^2} = -\rho_0 \frac{\partial q(x,y,z,t)}{\partial t} \tag{1}$$

where ∇^2 is the Laplacian operator, c_o is the sound velocity in the air, ρ_0 is the ambient density of the air, $p(x,y,z,t)$ represents the acoustic pressure at time t inside the car cabin, and q is the volume velocity per unit volume. For the case of a point source located at (x_o,y_0,z_0), $q(x,y,z,t)$ is given by:

$$q(x,y,z,t) = Q(t)\delta\left[(x,y,z)-(x_0,y_0,z_0)\right] \tag{2}$$

where $Q(t)$ is the volume velocity of the point source and δ is the three-dimensional Dirac Delta function. In addition, the plate and air cavity coupling interface $S_{p\text{-}c}$ and rigid wall surface S_r are, respectively, given by:

$$\frac{\partial p(x,y,z,t)}{\partial n} = -\rho_0 \frac{\partial^2 w(y,z,t)}{\partial t^2} \tag{3}$$

$$\frac{\partial p(x,y,z,t)}{\partial n} = 0 \tag{4}$$

where $w(y,z,t)$ denotes the flexural displacement of the plate. n denotes the normal outer direction of the air cavity surface. On the other hand, the differential equation governing the plate displacement

is given by:

$$D\nabla^4 w(y,z,t) + \rho h \frac{\partial^2 w(y,z,t)}{\partial t^2} = p(x,y,z,t) \tag{5}$$

where $D = (1/12)(Eh^3/(1- \nu^2))$ is the bending stiffness of the plate, E is Young's modulus, and ν is Poisson's ratio, ∇^4 is the biharmonic operator, ρ and h are, respectively, the density and thickness of the plate. The edges all around the plate are assumed to be simply supported boundary conditions, and they are expressed as the following boundary conditions:

$$w(0,z,t) = 0; \quad \frac{\partial^2 w(0,z,t)}{\partial y^2} = 0 \tag{6}$$

$$w(L_y,z,t) = 0; \quad \frac{\partial^2 w(L_y,z,t)}{\partial y^2} = 0 \tag{7}$$

$$w(y,0,t) = 0; \quad \frac{\partial^2 w(y,0,t)}{\partial z^2} = 0 \tag{8}$$

$$w(y,L_z,t) = 0; \quad \frac{\partial^2 w(y,L_z,t)}{\partial z^2} = 0 \tag{9}$$

The noise propagation from the acoustic source in an interior trim porous material is modeled by using the Johnson-Champoux-Allard equivalent fluid model (27-29), to reduce the number of degrees of freedom in the numerical porous material modeling. The revised wave equation with complex effective density and velocity to the angular frequency ω is given by:

$$\nabla^2 \frac{p_p}{\rho_{eff}} + \frac{\omega^2}{\rho_{eff} c_{eff}^2} p_p = 0 \tag{10}$$

where p_p is the complex pressure amplitude in the interior trim porous material, ρ_{eff} is the effective density and c_{eff} is the complex effective sound velocity; they are given by:

$$\rho_{eff} = \frac{\alpha_\infty \rho_o}{\phi}\left[1 + \frac{\sigma\phi}{j\omega\rho_o\alpha_\infty}\sqrt{1 + j\omega\frac{4\alpha_\infty^2\eta\rho_o}{\sigma^2\Lambda^2\phi^2}}\right] \tag{11}$$

$$c_{eff} = \sqrt{K(\omega)/\rho_{eff}} \tag{12}$$

where σ, α_∞, ϕ, Λ are, respectively, the air flow resistivity, the tortuosity, the porosity, the viscous characteristic length, η is the ambient air viscosity, and ρ_o is the density of the air. $K(\omega)$ is the effective bulk modulus; it is given by:

$$K(\omega) = \frac{P_o\gamma_o}{\gamma_o - (\gamma_o - 1)\left(1 + \frac{8\eta}{j\omega\rho_o P_{rt}\Lambda'^2}\sqrt{1 + j\omega\frac{\rho_o P_{rt}\Lambda'^2}{16\eta}}\right)^{-1}} \tag{13}$$

where γ_o is the specific heat ratio, P_o is the static reference pressure, P_{rt} is the Prandtl number for the ambient air fluid, and Λ' is the thermal characteristic length.

3.2 Finite element simulation model

The simulation model is uses the FE method, in which the standard finite element procedures are applied to the equilibrium equation mentioned above. Figure 3(b) shows an acoustic car cabin FE model with an interior trim porous material that is developed in this study. MSC Actran™ 17 software is used to implement and predict the acoustic properties of vehicle interior trim materials in the car cabin.

Several simulation examples are presented to validate the car cabin experiment model, and the effects of the interior trim materials on the sound pressure level are investigated. Figure 4 shows the developed car cabin simulation model for three different cases: one case had no interior trim materials, and the other two had a single layer/multilayer interior trim material applied to the inner surface of the aluminum plate. In this simulation, 2-D shell elements are used for modeling the thin flexible aluminum plate. The aluminum plate has the material properties of Young's Modulus E = 69.5 GPa,

Poisson's Ratio $\nu = 0.33$, and density $\rho = 2700$ kg/m^3. For modeling the interior trim materials and the car cabin air cavity, 3-D solid elements are used. The air properties are the density $\rho_0 = 1.18$ kg/m^3, and the speed of sound $c_0 = 346$ m/s. They are calculated based on the ambient temperature measured in the laboratory. The interior trim material properties are given in Table 1. The interfaces between each two components, e.g. the plate and air cavity interface $S_{p\text{-}c}$, the plate and interior trim interface $S_{p\text{-}i}$, the interior trim and air cavity interface $S_{i\text{-}c}$, must be defined, and they can be found in the MSC Actran™ 17 User's Guide. Moreover, the acoustic source is modelled by using a monopole, where the reference noise is obtained from the reference Mic#1 experiment data, and the analysis of the acoustic response is up to 1000 Hz.

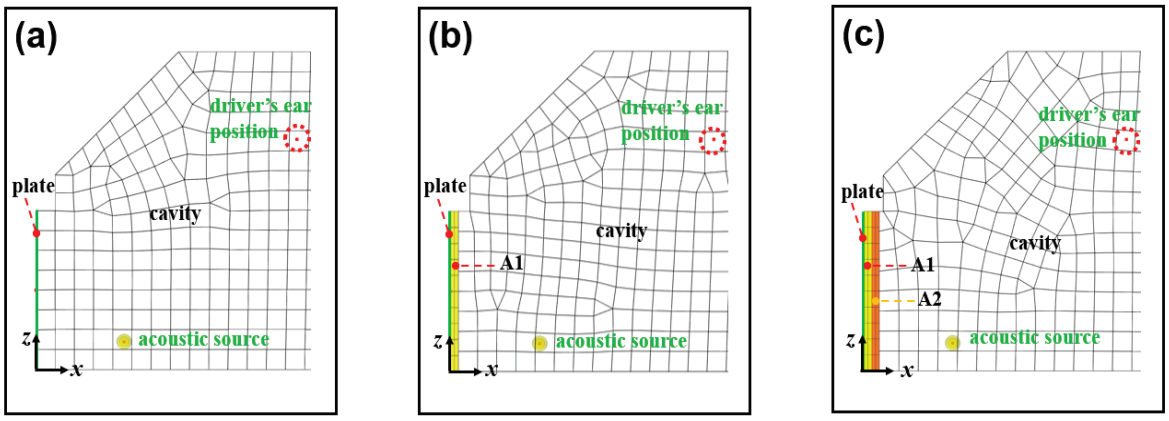

Figure 4 – FE model of car cabin including acoustic source and receiver: (a) without interior trim material; (b) with a single interior trim material; (c) with a multilayer interior trim material.

4. RESULTS AND DISCUSSION

4.1 Comparison of experiment and simulation

In this section, the FE simulation results and the experimental data are carefully compared and discussed. Figure 5 shows the comparison between the experimental data and the simulation results, for the car cabin model without interior trim materials at the locations of Mic#2 and Mic#3. The comparison between the experiment data and the simulation results for the car cabin with the interior trim materials (single layer/multilayer porous material) are shown in Figure 6 and Figure 7, respectively. There is a fairly good agreement between the simulation results and the corresponding experiment data: the predicted sound pressure level compares well with the experiment data, although slight discrepancy is observable at some anti-resonance frequencies below 600 Hz. However, the slight discrepancy between the simulation results and experiment data at the frequencies above 600 Hz is mainly due to the analysis limitation of the FE method. The shorter wavelengths at higher frequencies require extremely fine meshes for the acoustic FE model. In this study, the individual modes are clearly visible and well separated at the frequency below 600 Hz. The peak values of sound pressure level indicate that the acoustic energy is mainly depends upon the plate resonances and the car cabin air cavity resonances.

The quality of the experiment can be investigated from the coherences shown in Figure 5 to Figure 7. In this study, the coherences revealed that the input acoustic excitation and output sound pressure at measurement positions of Mic#2 and Mic#3 are well correlated. The coherences also indicate that the measurement starts to deteriorate at the frequencies of each peak sound pressure. Moreover, it should be noted that the damping in the simulation model for each peak acoustic pressure needs to be adjusted. The maximum damping of the aluminum plate is 3.5% and for the air in the car cabin is 1.5%. These values were chosen based on a comparison of the simulation results with experimental data.

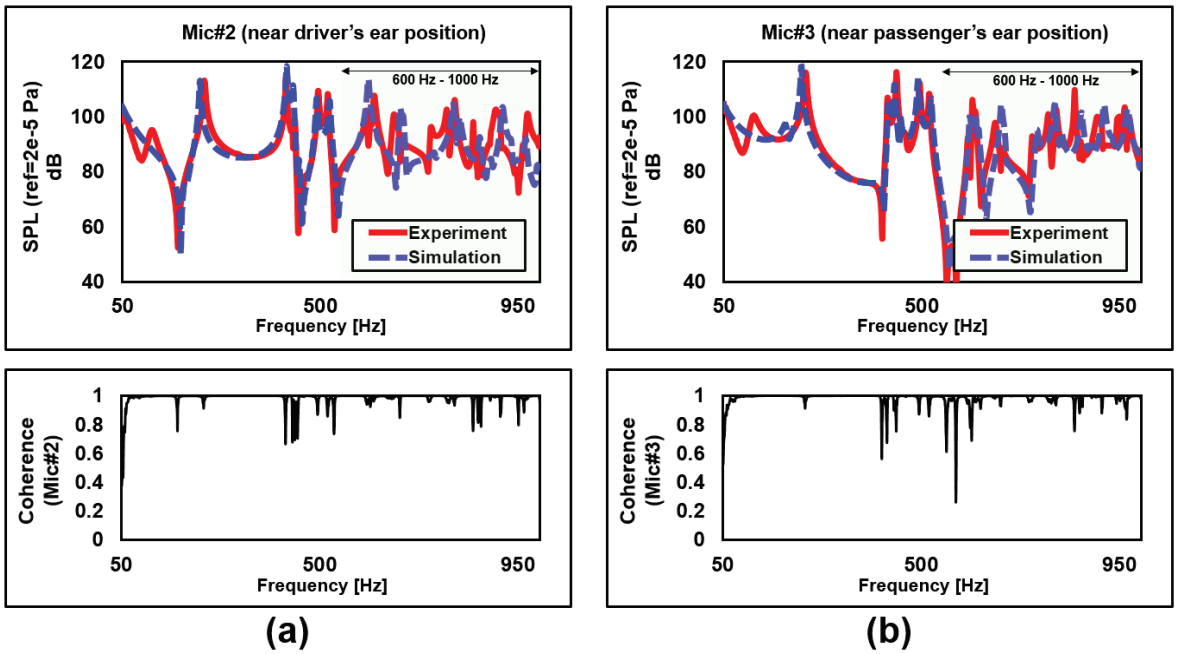

Figure 5 – Comparison of the acoustic response between the experiment data and simulation results for the car cabin model without interior trim, at the microphone location of (a) Mic#2 near the driver's ear position; (b) Mic#3 near the passenger's ear position. The results at the bottom show the coherences of microphone response at the two measurement positions.

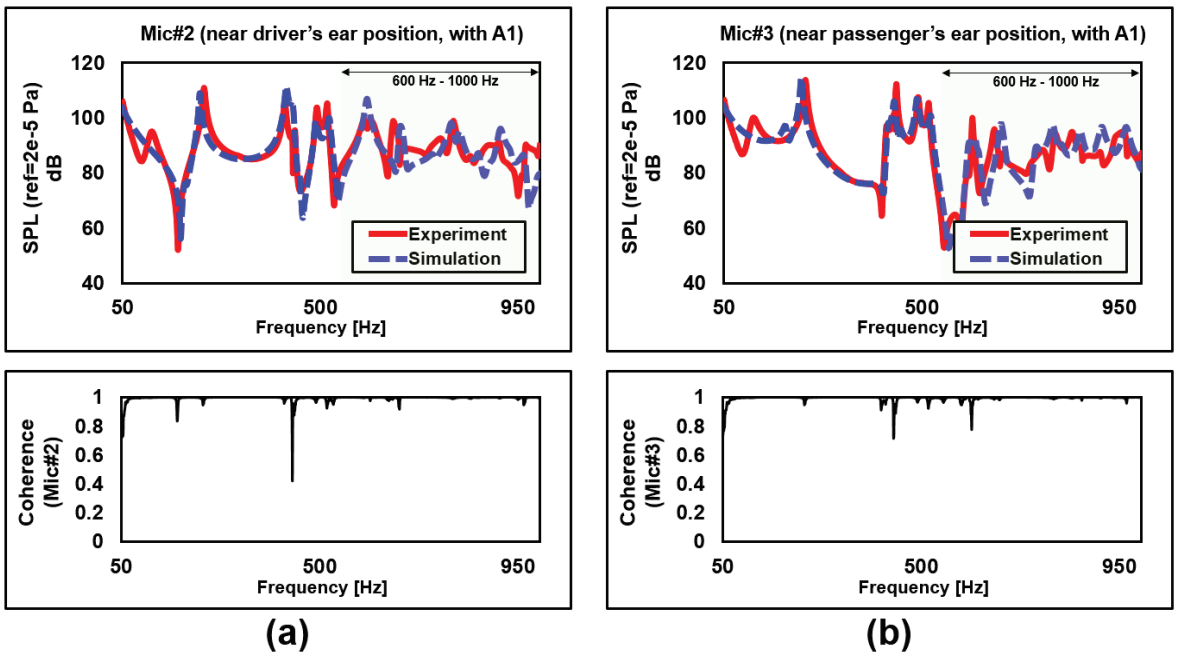

Figure 6 – Comparison of the acoustic response between the experiment data and simulation results for the car cabin model with a single interior trim material layer A1, at the microphone location of (a) Mic#2 near the driver's ear position; (b) Mic#3 near the passenger's ear position. The results at the bottom show the coherences of microphone response at the two measurement positions.

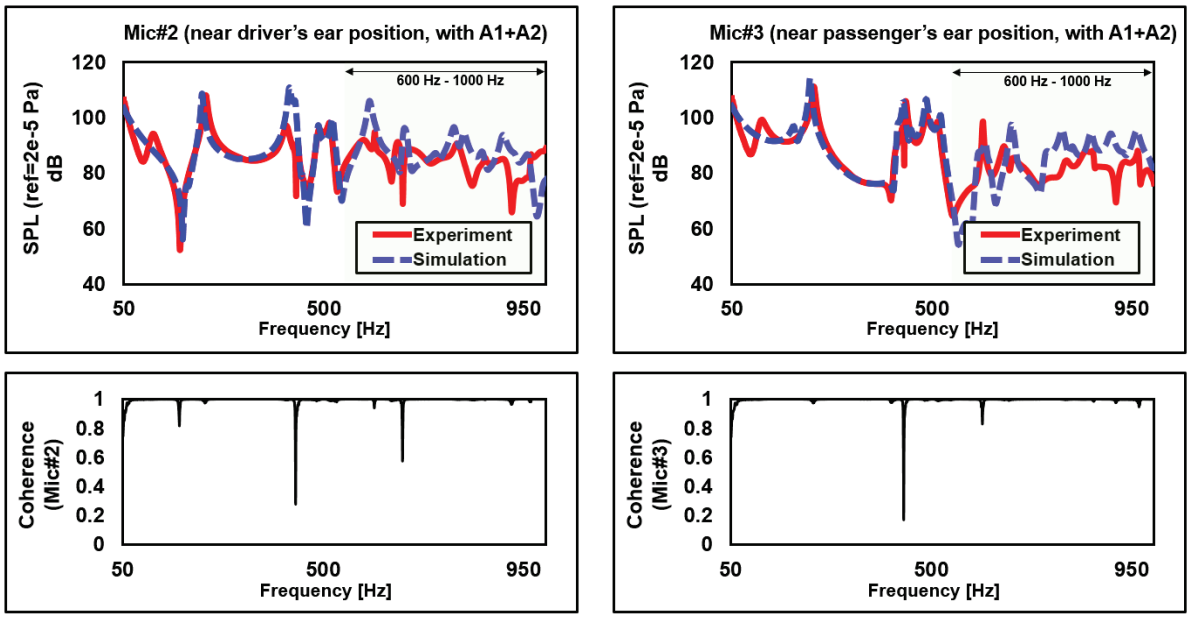

Figure 7 – Comparison of the acoustic response between the experiment data and simulation results for the car cabin model with a multilayer interior trim layer A1+A2, at the microphone location of (a) Mic#2 near the driver's ear position; (b) Mic#3 near the passenger's ear position. The results at the bottom show the coherences of microphone response at the two measurement positions.

4.2 Acoustic effects of interior trim materials

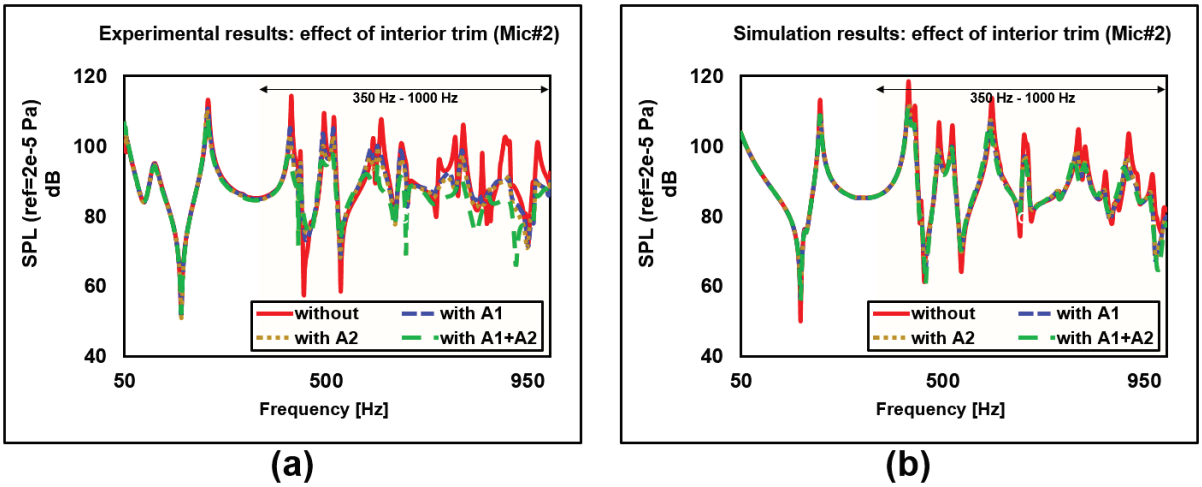

Figure 8 – Experimental (a) and (b) simulation results of the effect of the interior trims on the car cabin sound pressure level near the driver's ear position.

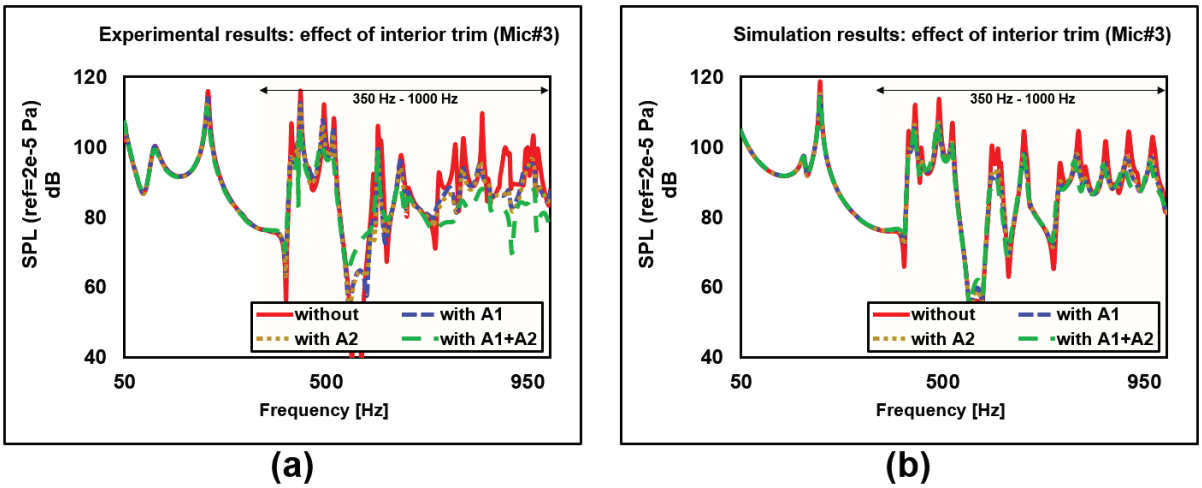

Figure 9 – Experimental (a) and (b) simulation results of the effect of the interior trims on the car cabin sound pressure level near the passenger's ear position.

Figure 8 and Figure 9 show the experimental and simulation results for the effect of the different cases of interior trim materials, on the sound pressure level of the car cabin near the driver's ear position and near the passenger's ear position, respectively. The results show that the interior trim materials reduce the airborne noise inside the car cabin, and provide a reduction of the sound energy at the modal frequencies compared to when the car cabin is not treated. At the frequencies below 350 Hz, the interior trim materials provide almost no attenuation of the airborne noise. The selected interior trim materials start to absorb the airborne noise effectively at frequencies above 500 Hz. The interior trim material A1 and A2 have almost the same acoustic properties in the frequency range between 50 Hz and 1000 Hz, even though interior trim material A2 has much lower mass than interior trim material A1. The experimental results show that the multilayer porous interior trim (A1+A2) structure provides a significant improvement in the noise reduction in the frequency range from 350 Hz to 1000 Hz. However, the thickness of the multilayer interior trim structure is almost double that of the single interior trim material layer. Moreover, as shown in the figures, the experimentally obtained results of the effect of the interior trims on the noise level inside a car cabin are more obvious. There must have been a small air gap between the plate and the porous interior trim material.

5. CONCLUSIONS

This paper presents an experimentally validated car cabin model to characterize the acoustic effect of vehicle interior trim materials in reducing the sound pressure level due to acoustic excitations. A scaled down car cabin model of a plate and cavity coupled system is used to investigate the acoustic effect of the interior trim materials on the car cabin noise level. The experimental data compare well with the simulation results both for the case of without and with single layer/multilayer interior trim material. The simulation and experimental results presented demonstrate the effectiveness of the proposed scaled down car cabin model in predicting the noise attenuation. The measured coherences demonstrate that the developed experiment method quality is maintained between 50 Hz and 1000 Hz for acoustical excitation. Future research will focus on the prediction of the acoustic properties of vehicle interior trim materials on a coupled plate and cavity system at higher frequencies, as well as optimizing its acoustic properties while reducing the weight, thickness, and cost.

ACKNOWLEDGEMENTS

The authors would like to thank Excellerate Australia Ltd and Futuris Automotive Group for their financial support for this research. The authors wish to acknowledge the technical staff at RMIT University (School of Engineering), Mr. Patrick Wilkins, Mr. Peter Tkatchyk and Mr. Julian Bradler in preparing a series of specimens and experiments. The authors are also thankful to Alias Isa, Tony Dong from MSC Software for their support. Zhengqing Liu is grateful to Master's degree student Wenhan Zhang, Jingyuan Tan and Wangke Hu for their assistance during the experiment.

REFERENCES

1. Sung SH, Nefske DJ. A coupled structural-acoustic finite element model for vehicle interior noise analysis. ASME Trans. 1984;106(2):314-318.
2. Citarella R, Federico L, Cicatiello A. Modal acoustic transfer vector approach in a FEM-BEM vibro-acoustic analysis. Eng Anal Bound Elem. 2007;31:248-258.
3. Courtois T, Bertolini C, Ochs J. A Procedure for efficient trimmed body FE simulations, based on a transfer admittance model of the sound package. Int J Passeng Cars-Mech Syst. 2010;3(2):1-13.
4. Kobayashi N, Habuchi M, Yamaoka H. FEM system development for dynamic response analysis of acoustic trim. Int J Passeng Cars-Mech Syst. 2009;2(1):1487-1493.
5. Zhou Z, Jacqmot, J, Vo TG, Jeong C, et al. Evaluation of trim absorption to exterior dynamic and acoustic excitations using a hybrid physical-modal approach. Int J Passeng Cars-Mech Syst. 2014;7(3):1205-1211.
6. Dowell EH, Voss HM. The effect of a cavity on panel vibration. AIAA J. 1963;1(2):476-477.
7. Dowell EH, Gorman GF, Smith DA. Acoustoelasticity: general theory, acoustic natural modes and forced response to sinusoidal excitation, including comparisons with experiment. J Sound Vib. 1977;52(4):519-542.
8. Pretlove AJ. Free vibrations of a rectangular panel backed by a closed rectangular cavity. J Sound Vib. 1956;2(3):197-209.
9. Pretlove AJ. Forced vibrations of a rectangular panel backed by a closed rectangular cavity. J Sound Vib. 1956;3(3):252-261.
10. Pretlove AJ, Craggs A. A simple approach to coupled panel-cavity vibrations. J Sound Vib. 1970;11(2):207-215.
11. Pan J, Bies DA. The effect of fluid-structural coupling on sound waves in an enclosure-Theoretical part. J Acoust Soc Am. 1990;87(2):691-707.
12. Pan J, Bies DA. The effect of fluid-structural coupling on sound waves in an enclosure-Experimental part. J Acoust Soc Am. 1990;87(2):708-717.
13. Lee YY. Structural-acoustic coupling effect on the nonlinear natural frequency of a rectangular box with one flexible plate. Appl Acoust. 2002;63(11):1157-1175.
14. Li YY, Cheng L. Vibro-acoustic analysis of a rectangular-like cavity with a tilted wall. Appl Acous. 2006;68:739-751.
15. Tanaka N, Takara Y, Iwamoto H. Eigenpairs of a coupled rectangular cavity and its fundamental properties. J Acoust Soc Am. 2012;131(3):1910-1921.
16. Du JT, Li WL, Liu, ZG, Xu HA, Ji ZL. Acoustic analysis of a rectangular cavity with general impedance boundary conditions. J Acoust Soc Am. 2011;130(2):807-817.
17. Du JT, Li, WL, Xu HA, Liu ZG. Vibro-acoustic analysis of a rectangular cavity bounded by a flexible panel with elastically restrained edges. J Acoust Soc Am. 2012;131(4):2799-2810.
18. Xin FX, Lu TJ. Analytical and experimental investigation on transmission loss of clamped double panels: Impedance of boundary effects. J Acoust Soc Am. 2009;125(3):1506-1517.
19. Liu F, Fang B, Kelkar AG. Energy extraction-based robust linear quadratic Gaussian control of acoustic-structure interaction in three-dimensional enclosure. J Vib Acoust. 2014;136(4):1-8.
20. Yang C, Cheng L. Sound absorption of microperforated panels inside compact acoustic enclosures. J Sound Vib. 2016;360:140-155.
21. Yamamoto T, Maruyama S, Nishiwaki S, Yoshimura M. Thickness optimization of a multilayered structure on the coupling surface between a structure and an acoustic cavity. J Sound Vib. 2008;318(1-2):109-130.
22. Kang SW, Lee JM. Structural-acoustic coupling analysis of the vehicle passenger compartment with the roof, air-gap, and trim boundary. J Vib Acoust. 2000;122:196-202.
23. Atalla N, Amédin CK, Sgard F. Numerical and experimental investigation of the vibro-acoustics of a

plate backed cavity coated with an heterogeneous porous material. SAE Technical Paper. 2003-01-1453, doi:10.4271/2003-01-1453.
24. Bécot FX, Sgard F. On the use of poroelastic materials for the control of the sound radiated by a cavity backed plate. J Acoust Soc Am. 2006;120(4):2055-2066.
25. Bécot FX, Jaouen L, Sgard, F. Noise control strategies using composite porous materials-Simulations and experimental validations on plate/cavity systems. Noise Control Engin J. 2011;59(5):464-475.
26. Allard JF, Champoux Y. New empirical equations for sound propagation in rigid frame fibrous materials. J Acoust Soc Am. 1992;91(6):3346-3353.
27. Johnson DL, Koplik J, Dashen R. Theory of dynamic permeability and tortuosity in Fluid-saturated porous media. J Fluid Mech. 1987;176:379-402.
28. Champoux Y, Allard JF. Dynamic tortuosity and bulk modulus in air-saturated porous media. J Appl Phys. 1991;70(4):1975-1979.
29. Atalla N, Panneton R. The effect of multilayer sound-absorbing treatments on the noise field inside a plate backed cavity. Noise Control Engin J. 1996;44(5):235-243.
30. Liu Z, Fard M, Davy JL. Prediction of the effect of porous sound-absorbing material inside a coupled plate cavity system. Int J Vehicle Noise Vib. 2016;12(4):314-330.
31. Liu Z, Fard M, Davy JL. The effects of porous materials on the noise inside a box cavity. Proc 22nd International Congress on Sound and Vibration; 12-16 July 2015; Florence, Italy 2015. p. 1-8.
32. Liu Z, Fard M, Davy JL. Acoustic properties of the porous material in a car cabin model. Proc 23rd International Congress on Sound and Vibration; 10-14 July 2016; Athens, Greece 2016. p. 1-8.
33. Liu Z, Fard M, Jaza R. Development of an acoustic material database for vehicle interior trims. Proc 18th Asia Pacific Automotive Engineering; 10-12 March 2015; Melbourne, Australia 2015. p. 1-7.